CHAPTER IV
RESULTS AND DISCUSSION

4.1 Catalyst Characterization

4.1.1 Elemental Analysis by XRF

Table 4.1 shows the chemical compositions obtained from XRF analyses, expressed as weight percentages, of the investigated catalysts. As mentioned in methodology, the theoretical Ce/Zr mole ratio is 3/1. The fixed Ni content is 15 wt% whereas Mg content is varied in the range of 1-6 wt% of the catalyst. When compared between measured and theoretical values, all values remain consistent and close to the theoretical ones.

Table 4.1 Elemental analysis results for the catalysts synthesized

Catalyst	Compositions (wt%)					Mole ratio of Ce/Zr
	Ce	Zr	Ni	Mg	O	
CZO	67.04	13.06	n/a	n/a	19.90	3.34/1
15Ni/CZO	50.88	11.25	17.52	n/a	20.35	2.72/1
Ni-1%Mg/CZO	50.31	11.49	16.61	0.93	20.66	2.94/1
Ni-3%Mg/CZO	48.76	9.13	17.72	3.15	21.24	2.85/1
Ni-6%Mg/CZO	50.15	10.95	17.68	6.55	14.67	2.98/1
1%Mg-Ni/CZO	47.69	11.96	18.71	0.88	20.76	2.60/1
3%Mg-Ni/CZO	47.99	10.72	17.2	2.82	21.27	2.91/1
6%Mg-Ni/CZO	45.55	9.85	15.88	6.28	22.44	3.01/1

4.1.2 BET Surface Area and Degrees of Metal Dispersion

BET surface areas and degree of metal dispersion of the investigated catalysts are shown in Table 4.2. The surface area of $Ce_{0.75}Zr_{0.25}O_2$ (CZO) support was ca. 89.78 m^2/g whereas that of Ni/ CZO was 62.745 m^2/g. By loading Ni metal onto CZO support, the CZO surface area was found to decrease by about 30.11%. This might be due to nickel could perform as a nucleating agent to promote the sintering over CZO supported catalysts (Montoya *et al.*, 2000).

Table 4.2 BET surface areas and degrees of metal dispersion of the catalysts

Catalyst	BET surface area (m^2/g)	Metal dispersion (%)	Surface area of Ni (m^2/g)
CZO	89.78	n/a	n/a
Ni/CZO	62.75	5.86	0.29
6%Mg/CZO	18.95	n/a	n/a
Ni-1%Mg/CZO	55.52	3.65	0.18
Ni-3%Mg/CZO	49.71	2.49	0.12
Ni-6%Mg/CZO	47.49	1.51	0.08
1%Mg-Ni/CZO	51.91	3.38	0.17
3%Mg-Ni/CZO	36.90	0.89	0.05
6%Mg-Ni/CZO	29.15	0.69	0.03

As the amount of Mg increased from 1 to 6wt%, the surface area decreased. This might be due to the pore blockage of MgO (Yejun *et al.*,2007). The decrease in the surface area decreased the number of active sites exposed to the chemical atmosphere (Ruckenstein and Hu *et al.*, 1999). Thus, Mg containing

catalysts should have lower amount of NiO exposed to the chemical reaction resulting in lower catalytic activity of the catalysts.

For Ni-Mg/CZO catalysts(CZO support impregnated with Mg following by Ni), the specific surface areas of Ni-1%Mg/CZO, Ni-3%Mg/CZO, Ni-5%Mg/CZO were 55.5, 49.7 and 47.5 m^2/g, respectively, all of which were lower than that of Ni/CZO. The surface areas of those catalysts were slightly decreased with increasing Mg content, probably due to the pore blockage of Mg (Yejun *et al.*, 2007).

For Mg-Ni/CZO catalysts (CZO support impregnated with Ni following by Mg), the surface areas were found to decrease drastically with increasing Mg loading. In this case, it might be due to after impregnate Ni, Ni has the strong interaction with CZO support. Consequently, Mg has less interaction with Ni and then tends to aggrumulate at the entrance of pore resulting in the pore blockage of MgO.

The metal dispersions were found to decrease with increasing Mg loading. Since no hydrogen chemisorption is observed over the CZO and MgO/CZO, this indicates that Ni atoms being exposed to H_2 were partially covered by MgO.

At given loading of Mg, both surface areas and metal dispersion of Ni-Mg/CZO were higher than those of Mg-Ni/CZO. This indicates that the metal incorporated sequence significantly affects the properties of catalysts.

4.1.3 X-ray Diffraction (XRD)

XRD patterns for the NiO-MgO over CZO catalysts are shown in Figure 4.1. All the catalysts exhibited major peaks at ca. 28.8°, 33.5°, 47.5°, and 56.8° (2θ) indicating a cubic fluorite structure of CeO_2 (Pengpanich *et al.*, 2002). Small peaks of NiO were observed at ca. 37.2°, 43.3°, 63.0°, and 79.0° (2θ). No distinguishable peaks of MgO could be observed for the catalysts prepared. This might be due to the similar characteristics of XRD patterns for both NiO and MgO (Tang *et al.*, 1998) and/or the small amount of Mg loading.

As compared with the diffraction peaks of Ni/CZO, an increase in MgO loading resulted in a slightly decrease NiO peaks indicated above. However, the NiO diffraction peaks at ca. 43.3°(2θ) of both metal incorporated sequences

shifted to the lower degree with increasing the content of Mg, indicating the formation of Ni-Mg mixed oxide solid solution.(Yejun *et al.*, 2007).

Because NiO peaks overlap with MgO peaks, it is not possible to calculate the NiO size using Shcerrer equation (Roh *et al.*, 2007).

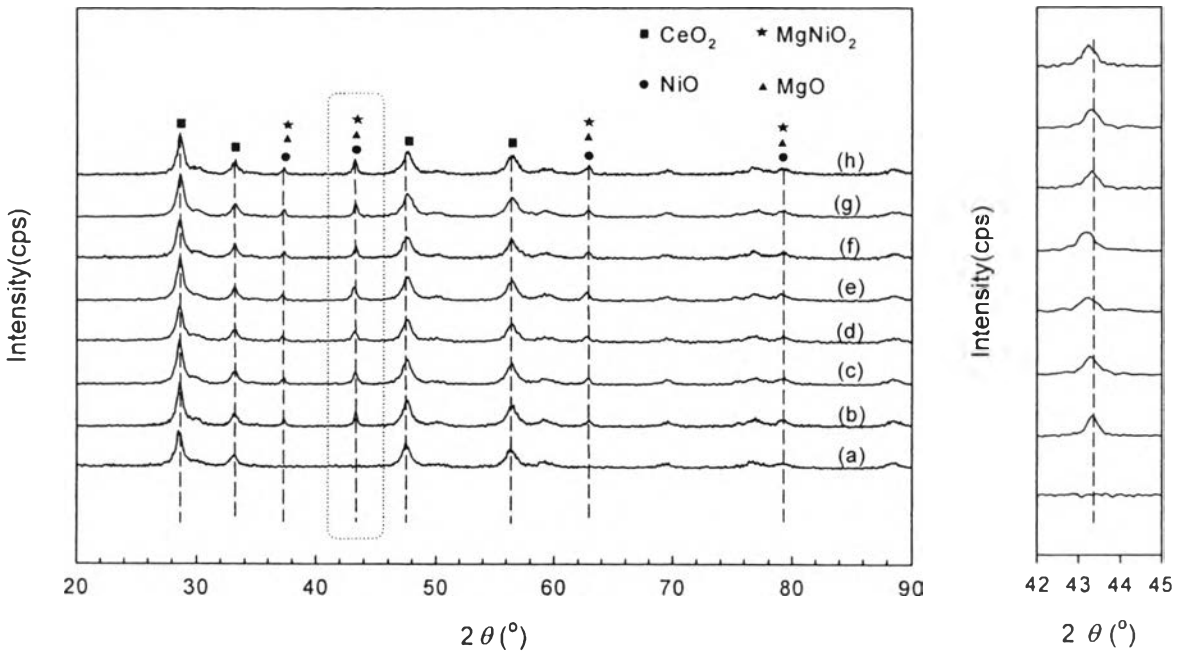

Figure 4.1 XRD patterns of the catalysts: (a) CZO, (b) Ni/CZO, (c) Ni-1%Mg/CZO, (d) Ni-3%Mg/CZO, (e) Ni-6%Mg/CZO, (f) 1%Mg-Ni/CZO, (g) 3%Mg-Ni/CZO, and (h) 6%Mg-Ni/CZO.

4.1.4 Temperature-programmed Reduction by Hydrogen (H_2-TPR)

H_2-TPR profiles for the catalysts investigated are presented in Figure 4.2. The TPR profile for CZO indicates a typical reduction peak of CeO_2 at ca. 550 °C. The Ni/CZO catalyst possesses two reduction peaks at ca. 265 and 350 °C, and one shoulder peak at about 500 °C. This suggests that there are two kinds of NiO species. The low temperature peak is assigned to a free NiO species interacting weakly with the support, and the another peak at higher temperature is attributed to a complex NiO species interacting strongly with the support (Roh *et al.*, 2002).

Furthermore, the shoulder peak corresponds to CeO_2 which shifts downward, and then overlaps the NiO reduction peak at about 500°C (Dong *et al.*,

2002). This indicates that a strong interaction between Ni and $CeZrO_2$ makes ceria more reducible.

Effect of incorporating Mg onto the Ni/CZO catalysts on the reducibility of nickel species was observed for which the reduction temperatures of NiO were virtually increased in various degrees depending on both of its amount and incorporated sequences. The presence of MgO might cause an interaction between NiO and MgO and/or an intervention of the interaction between NiO and CZO resulting in a more difficulty in NiO reducibility. Another explanation is the most reactive forms of NiO had undergone a progressive diffusion into MgO lacttice and likely formed a NiO-MgO solid solution (Wen *et al.*, 2011). The rise of reduction temperature with increasing Mg loading implies the NiO is better protected by MgO because of more MgO present in the solid solution (Yin *ei al.*, 2011).

Obviously, the intensity of reduction peaks at high temperature region (350°C) for both Ni-Mg/CZO and Mg-Ni/CZO catalysts were lower than Ni/CZO, indicating the lower amount of fixed NiO which has strong interaction with support. Both NiO and MgO have a face-centered cubic structure with almost the same lattice parameters and bond distances (Hu and Ruckenstein *et al.*, 1995). For this reason, MgO and NiO can form solid solutions. This was demonstrated both by the XRD and TPR results.

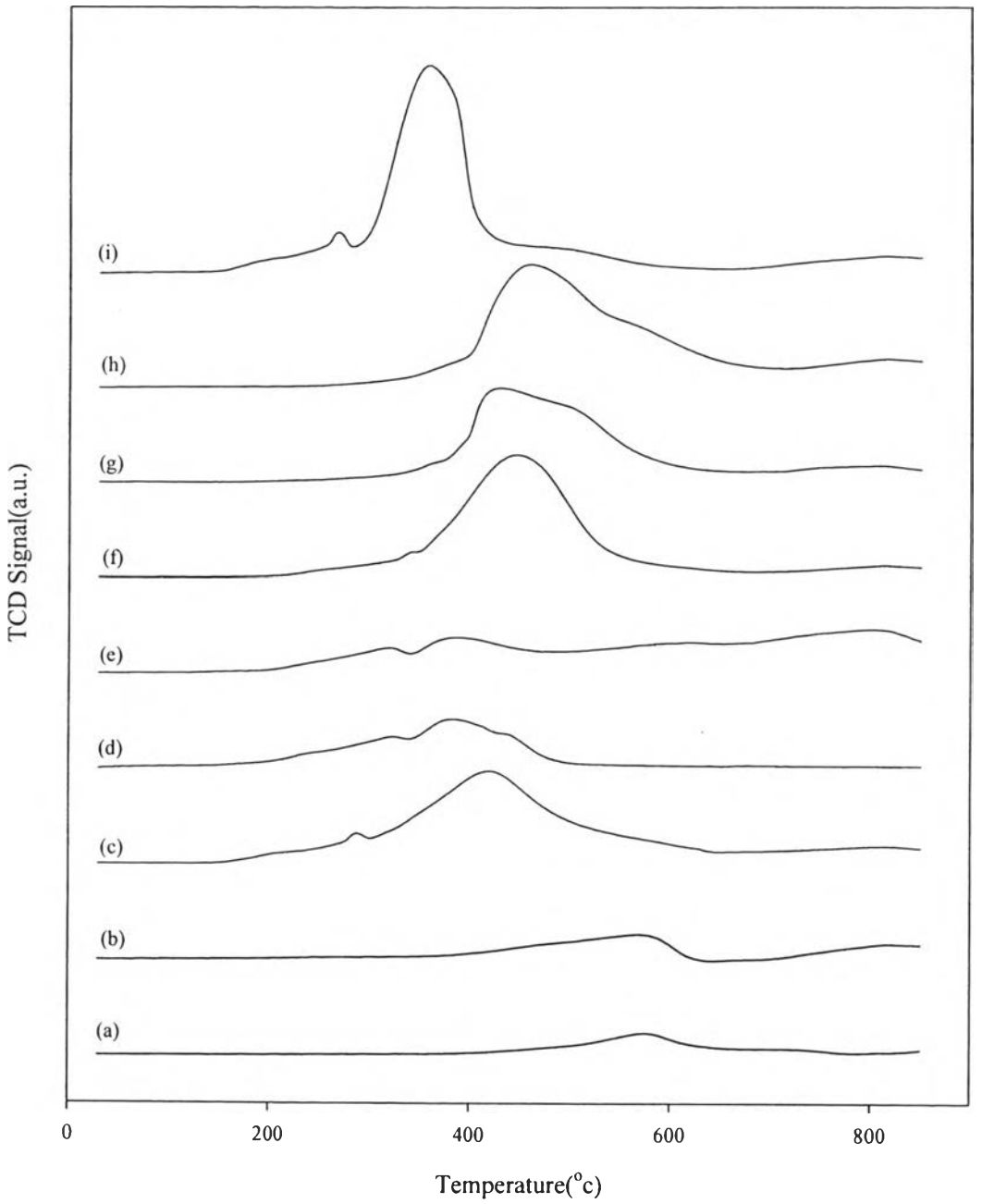

Figure 4.2 H_2-TPR profiles for the catalysts with a heating rate of 10 °C min^{-1}, a reducing gas containing 5% hydrogen in argon with a flow rate of 10 ml min^{-1}: (a) 6%Mg/CZO, (b) CZO, (c) Ni-1%Mg/CZO, (d) Ni-3%Mg/CZO, (e) Ni-6%Mg/CZO, (f) 1%Mg-Ni/CZO, (g) 3%Mg-Ni/CZO, (h) 6%Mg-Ni/CZO, and (i) Ni/CZO.

Figure 4.3 shows the H_2-TPR results of the catalysts in each metal incorporated sequence. As illustrated in Fig.4.3 (a), the second reduction peak intensity of Ni-Mg/CZO catalyst at ca. 350°C decreased drastically with the rise of Mg content indicating lower amount of NiO in intimate contact with the oxide support. This might be due to the formation of NiO-MgO solid solution. This might be postulated that the weak interaction between Mg and CZO resulting in easier forming NiO and MgO solid solution.

In TPR profiles of Mg-Ni/CZO catalysts shown in Fig.4.3 (b), the reduction peak intensity of Mg-Ni/CZO catalyst decreased slightly with increasing Mg content and shifted to higher temperature. These results suggest that when Ni loading first followed by Mg, NiO particles were mostly covered by MgO. Thus, MgO particles required high temperature to mobilize from covering NiO particles and then NiO could expose to H_2 atmosphere.

Figure 4.4 presents the H_2-TPR results of the catalysts when compared between each sequence. At a given loading of Mg, the reduction temperature of Ni-Mg/CZO catalyst was lower than that of Mg-Ni/CZO, indicating that NiO in Ni-Mg/CZO is easier to be reduced. Besides, the first reduction peak intensity of Ni-Mg/CZO at ca. 265°C was higher than that of Mg-Ni/CZO. Conversely, the second reduction peak intensity of Ni-Mg/CZO at ca. 350 °C was lower than that of Mg-Ni/CZO catalyst. These results indicate that Ni-Mg/CZO catalyst has a higher amount of free NiO species interacting weakly with support due to Mg hinder the interaction between Ni and CZO whereas has a lower amount of complex NiO species interacting strongly with support due to NiO and MgO solid solution. It was reported that free NiO species, which has weak interaction with support is responsible for coke formation (Roh *et al.*, 2007). The more free NiO species, the higher quantity of coke. Thus, the Ni-Mg/CZO catalyst may have more active but poorer coke resistant.

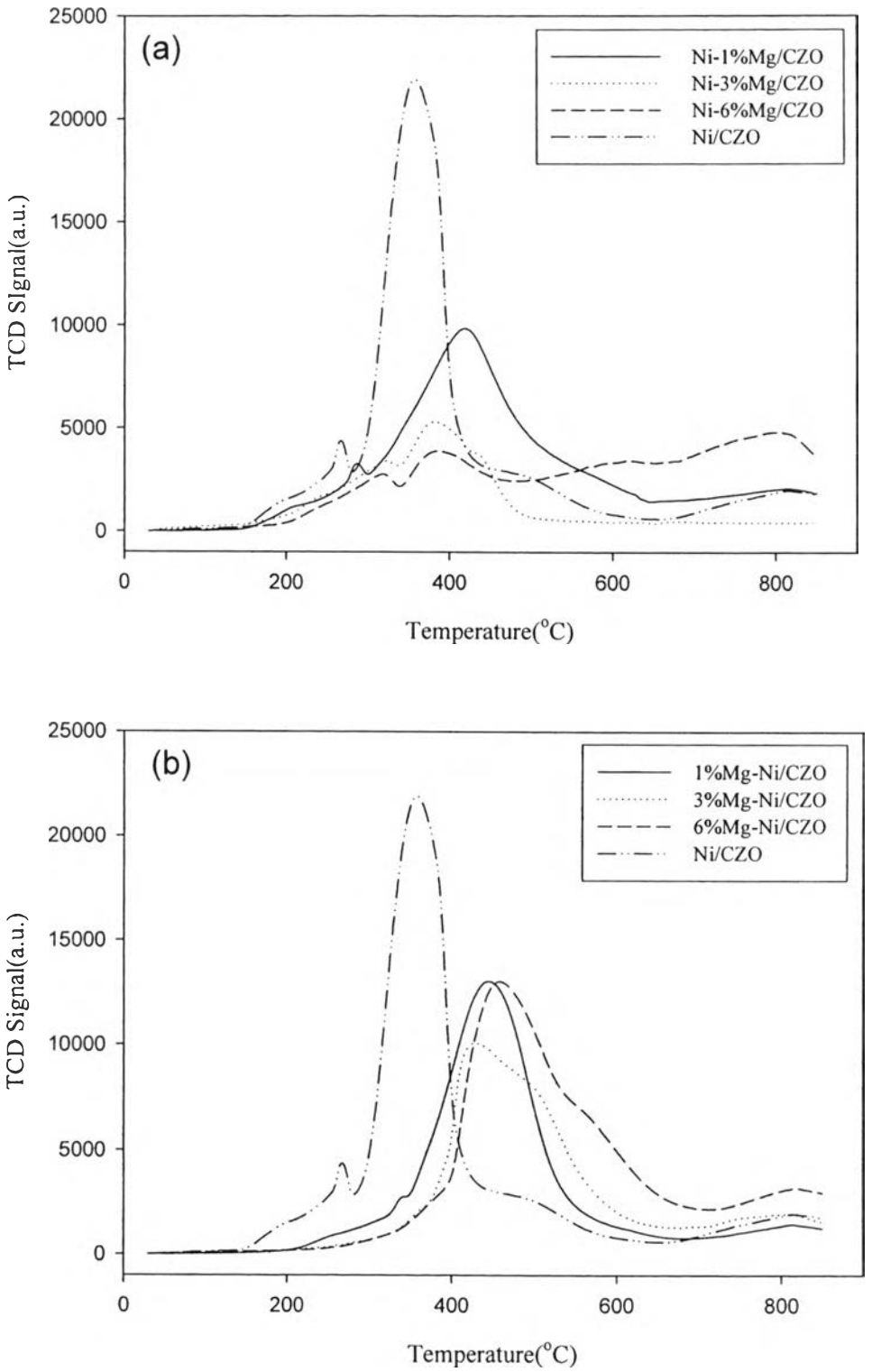

Figure 4.3 H_2-TPR profiles for the catalysts with a heating rate of 10 °C min^{-1}, a reducing gas containing 5% hydrogen in argon with a flow rate of 10 ml min^{-1}.

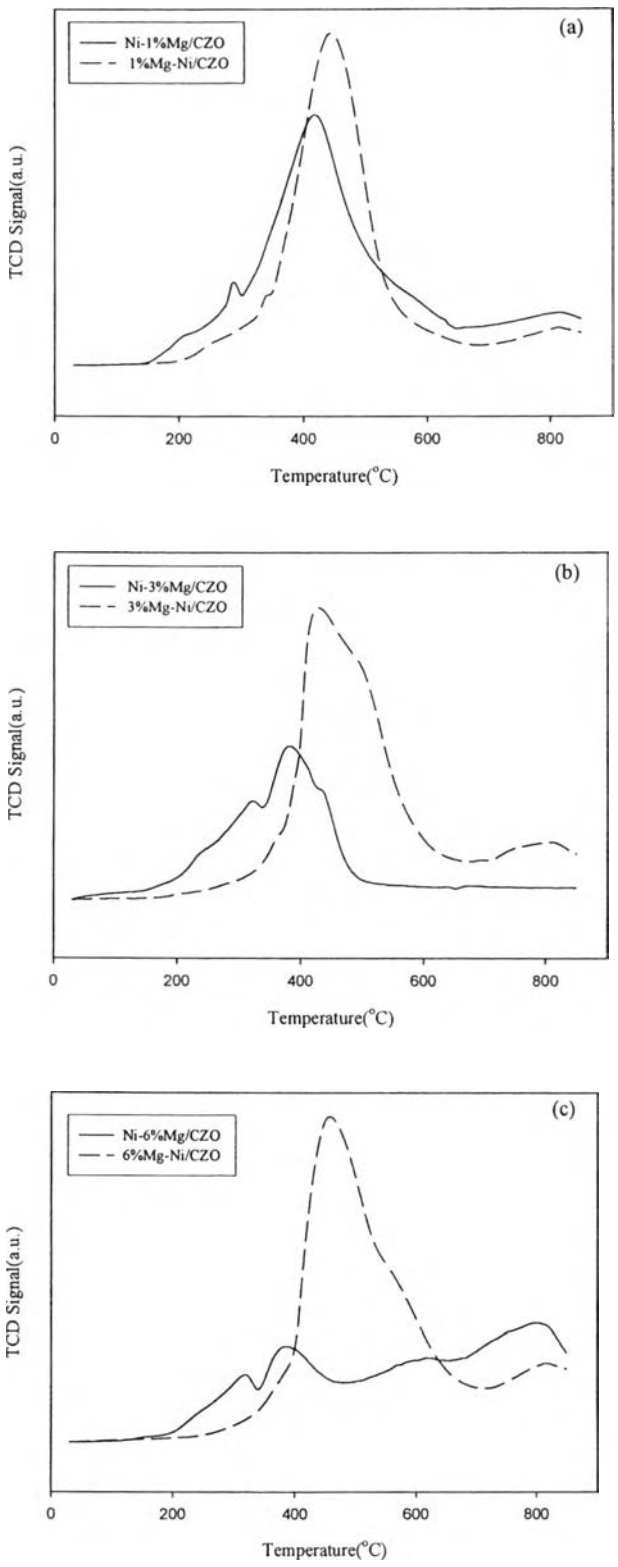

Figure 4.4 H_2-TPR profiles for the catalysts with a heating rate of 10 °C min^{-1}, a reducing gas containing 5% hydrogen in argon with a flow rate of 10 ml min^{-1}.

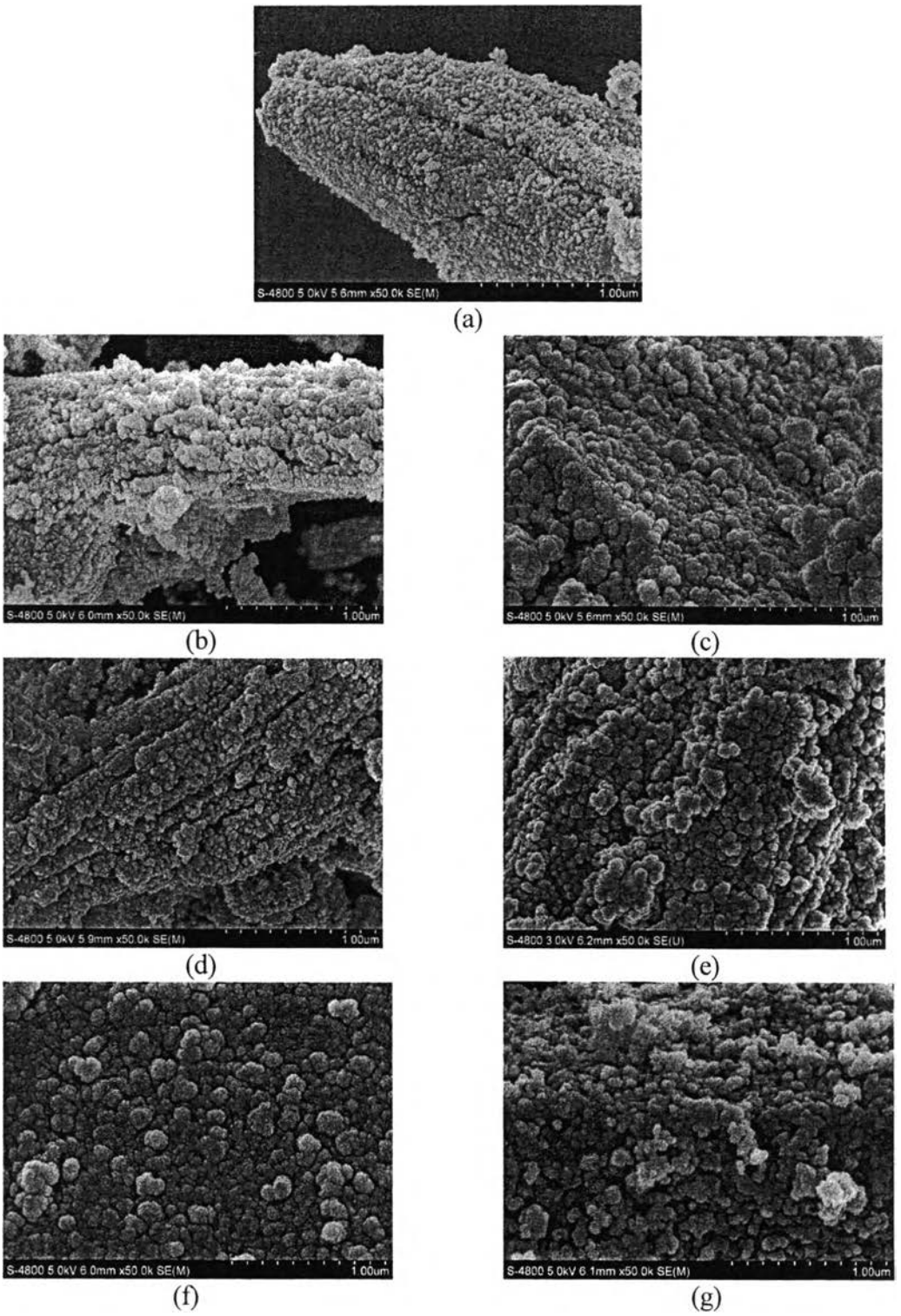

Figure 4.5 SEM images (50000x magnifications) of (a) Ni/CZO (b) Ni-1%Mg/CZO (c) 1%Mg-Ni/CZO (d) Ni-3%Mg/CZO (e) 3%Mg-Ni/CZO (f) Ni-6%Mg/CZO (g) 6%Mg-Ni/CZO

4.1.5 Scanning Electron Microscopy (SEM)

Figure 4.5 shows SEM images of all catalysts investigated. The NiO size of the Ni/CZO catalyst was in the range of 20-50 nm. For Mg containing catalysts, the metal oxide size of the sample was in the range of 30-80 nm. When compared Mg containing catalysts with Ni/CZO, particle size of Mg containing catalysts was larger than that of Ni/CZO. In addition, the increase of Mg content resulted in the aggregation of metal particles. This is in agreement with lower surface area and metal dispersion.

4.2 Catalytic Activities for Methane Partial Oxidation

4.2.1 Catalytic Activities for CPOM

Catalytic partial oxidation of methane (CPOM) was carried out over all catalysts under the following conditions: CH_4/O_2 ratio of 2:0, GHSV = 53000 h^{-1}. For the Ni/CZO catalyst, CPOM is initially started at a temperature of 550 °C.

For the Mg loading catalysts, CPOM is initially started at a temperature of 600 °C for 1 wt% Mg and shifted to higher temperatures with increasing Mg loading. This might be due to the NiO surface was partially covered with MgO and/or NiO and MgO mixed oxide solid solution can lead to the difficulty in reducing NiO resulting in less catalytic activity (Pue-on *et al.*, 2010).

At 1wt% of Mg loading, the light-off temperatures of both Ni-1%Mg/CZO and 1%Mg-Ni/CZO were started at same temperature (600°C). These results indicated that the metal incorporation of Mg and Ni does not seem to play a significant role in the catalytic activity when Mg loading is less than 1 wt%

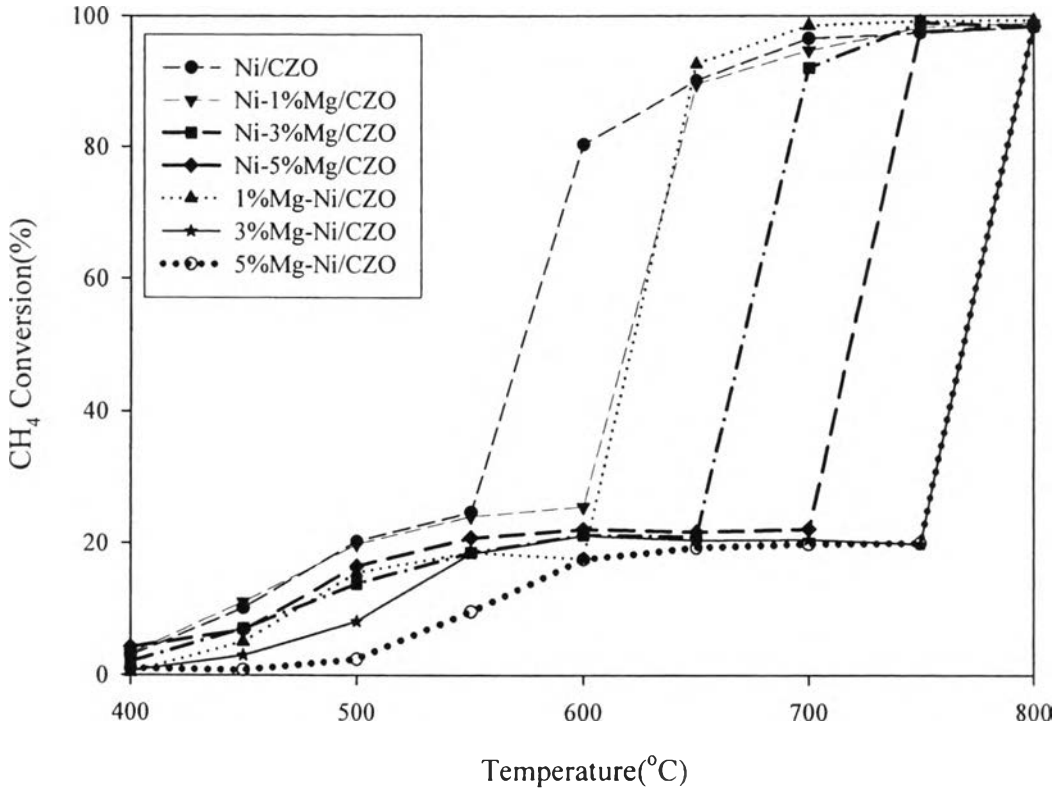

Figure 4.6 Methane conversion at different temperature over the investigated catalyst using CH_4/O_2 ratio = 2:1 and GHSV = 53000 h^{-1}.

For higher amount of Mg loadings (≥3 wt%), the light-off temperatures of the Ni-Mg/CZO catalysts were started at lower temperature than those of Mg-Ni/CZO catalysts. This might be due to NiO particles in Mg-Ni/CZO are more partially covered by MgO particles. Thus, NiO particles in Mg-Ni/CZO with ≥3 wt%Mg loading required a reduction temperature higher than 750°C. These results indicate that Mg-Ni/CZO catalyst has high activity in partial oxidation of methane. However, Mg-Ni/CZO which is not reduced enough was active for only methane combustion (Nurunnabi M. *et al.*, 2005).

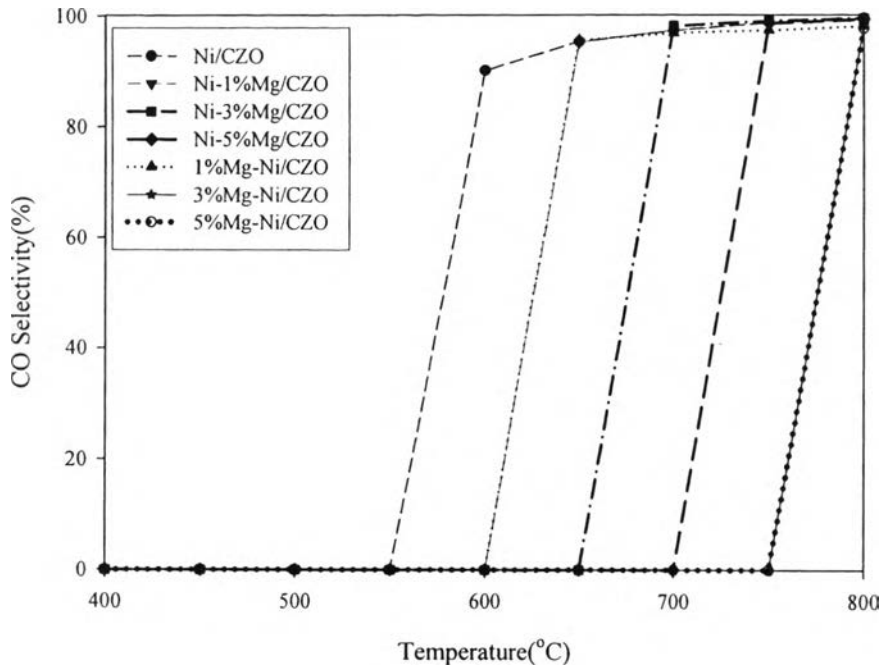

Figure 4.7 CO Selectivity at different temperature over the investigated catalyst using CH_4/O_2 ratio = 2:1 and GHSV = 53000 h^{-1}.

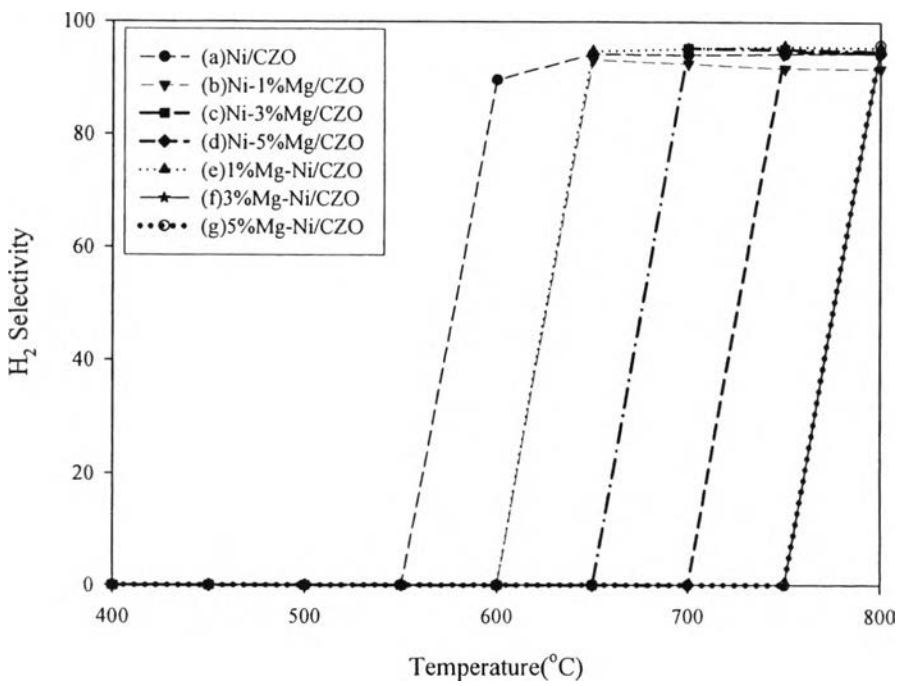

Figure 4.8 H_2 Selectivity at different temperature over the investigated catalyst using CH_4/O_2 ratio = 2:1 and GHSV = 53000 h^{-1}.

In spite of CH_4 conversion, CO selectivity were slightly increased when reaction temperature increase, while H_2 selectivity remained almost the same. However, as seen in Figure 4.7, the CO selectivity is slightly increased at temperatures beyond 650°C when adding Mg promoter. This implies that the addition of Mg promoter can stabilize the dispersion of Ni particles beneficial to prevent the carbon deposition at high temperatures.

4.2.2 Carbon Deposition on Catalysts and Catalyst Stability

Due to their higher catalytic activities as compared with the others, the catalysts with Mg loading ≤3wt% were selected to further investigate on carbon deposition and catalytic activity under specified reaction conditions.

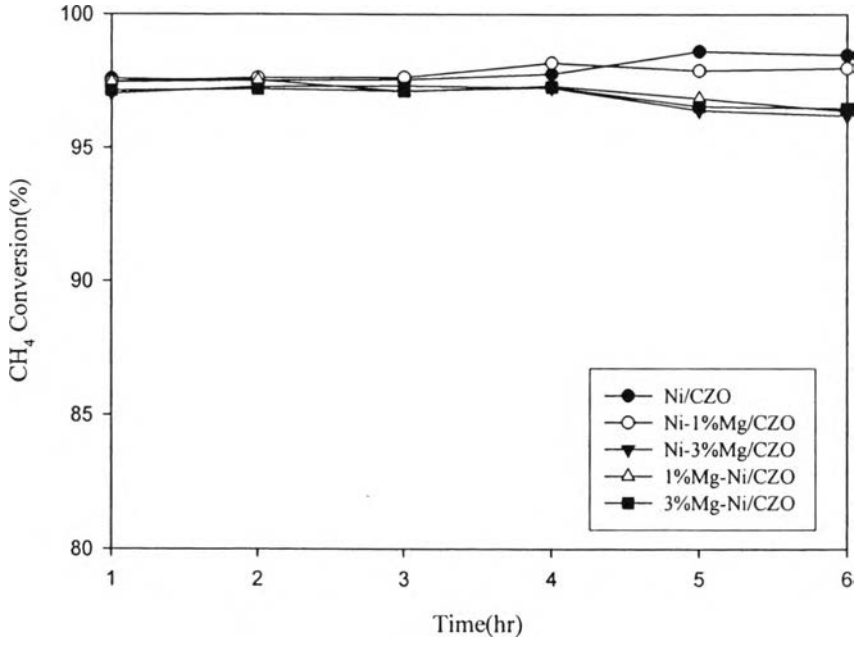

Figure 4.9 CH_4 conversion as a function of time over the catalysts investigated at 750°C (CH_4/O_2 ratio of 2:0, GHSV = 53000 h^{-1}).

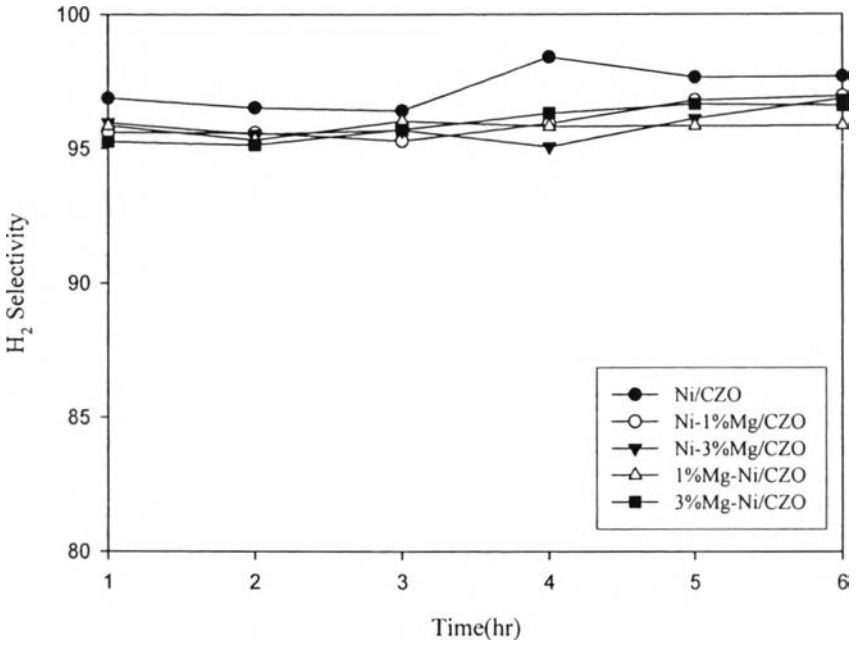

Figure 4.10 H_2 Selectivity as a function of time over the catalysts investigated at 750°C (CH_4/O_2 ratio of 2:0, GHSV = 53000 h^{-1}).

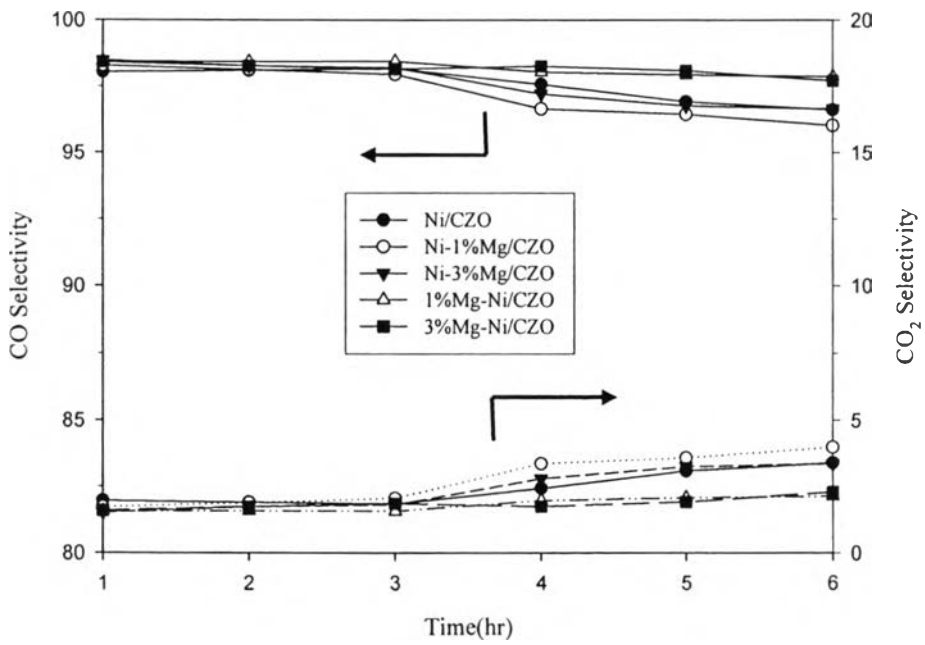

Figure 4.11 CO and CO_2 selectivities as a function of time over the catalysts investigated at 750°C (CH_4/O_2 ratio of 2:0, GHSV = 53000 h^{-1}).

Figures 4.9 - 4.11 illustrate the methane conversion, hydrogen selectivity, and carbon monoxide as well as carbon dioxide selectivity for the investigated catalysts, respectively. Accordingly, all the catalysts possessed insignificant variations in CH_4 conversion and H_2 selectivity. But, their CO selectivity is slightly decreased whereas CO_2 selectivity is slightly increased with increasing time on steam for MPO reaction at 750°C. This might be due to the CO oxidation ($CO + \frac{1}{2} O_2 \rightarrow CO_2$) might occur during the course of reaction.

Figure 4.12 presents the TPO profiles of the catalysts investigated after reaction at 750°C for 6 hrs. All the spent catalysts show peaks centered at about 370 and 720°C. It is suggested that the first peaks at temperature about 320°C could be described to amorphous carbon, and the second peaks at temperature about 720°C could be described to whisker carbon. The results are similar to that observed by Pengpanich *et al.* (2004) suggesting that the peaks observed on the TPO profiles can be due to the presence of different types of carbon or different sites of carbon deposition.

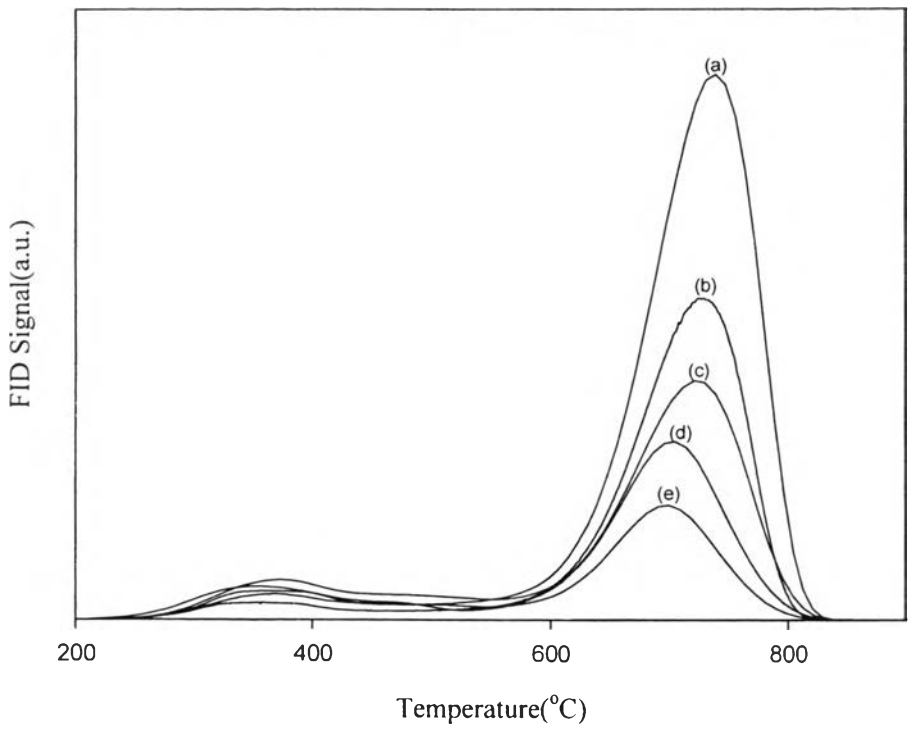

Figure 4.12 TPO profiles of catalysts after reaction at 750 °C (CH_4/O_2 of 2:0, GHSV = 53000 h^{-1}) an oxidizing gas containing 2% oxygen in He with a flow rate of 40 ml/min: (a) Ni/CZO (b) Ni-1%Mg/CZO (c) 1%Mg-Ni/CZO (d) Ni-3%Mg/CZO and (e) 3%Mg-Ni/CZO

As shown in Figure 4.13, the filamentous carbon was mainly formed on all spent catalysts. The results are in agreement with the main type of carbon deposition which was measured by TPO technique (Figure 4.12).

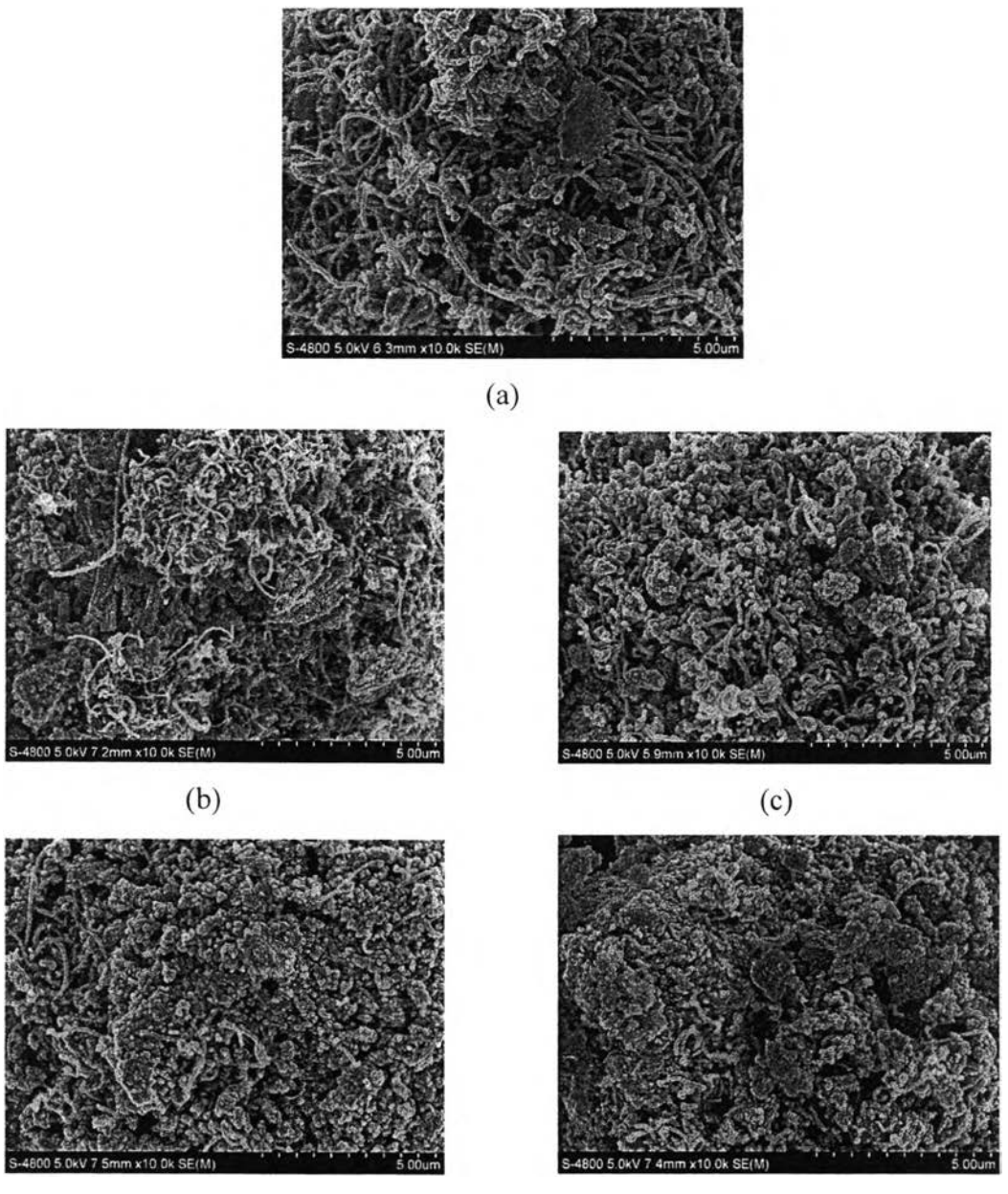

Figure 4.13 SEM images of filamentous carbon of (a) Ni/CZO (b) Ni-1%Mg/CZO (c) 1%Mg-Ni/CZO (d) Ni-3%Mg/CZO (e) 3%Mg-Ni/CZO spent catalysts after exposure to MPO reaction at 750°C (CH_4/O_2 = 2:0, GHSV = 53000 h^{-1}) for 6 hrs.

Figure 4.14 presents SEM images of the spent catalysts after exposure to MPO reaction at 750°C. The NiO particle size of the Ni/CZO catalyst was dramatically increased (100 – 200 nm) after a reaction time of 6 hours at 750°C whereas the NiO particle size of the Mg containing catalysts remained unchanged

(50-100 nm). It can be concluded that the addition of Mg at low Mg content could prevent the agglomeration of NiO particles at high temperatures.

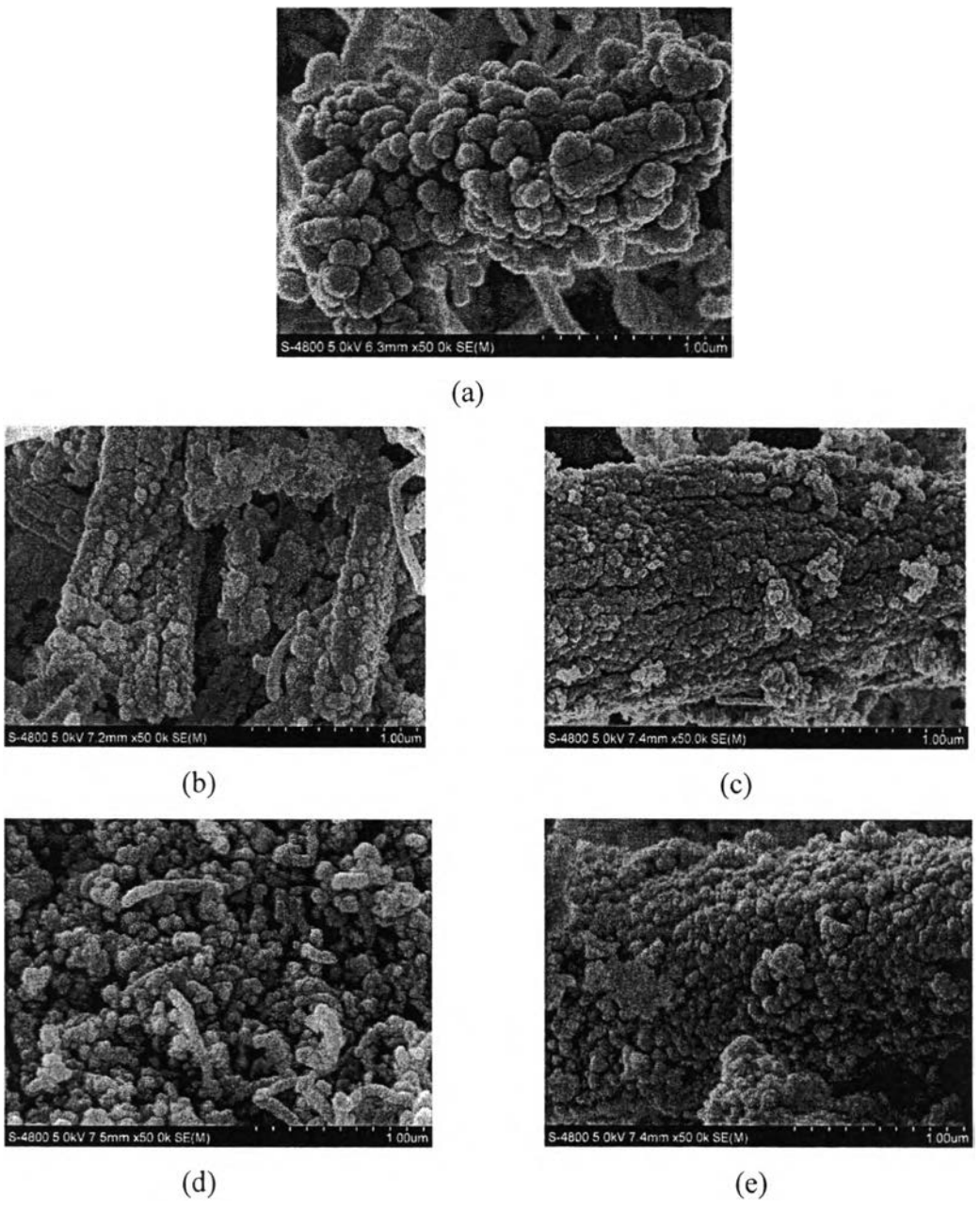

Figure 4.14 SEM images of (a) Ni/CZO (b) Ni-1%Mg/CZO (c) 1%Mg-Ni/CZO spent (d) Ni-3%Mg/CZO (e) 3%Mg-Ni/CZO catalysts after exposure to MPO reaction at 750°C (CH_4/O_2 = 2:0, GHSV = 53000 h^{-1}) for 6 hrs.

Table 4.3 The amount of carbon deposition measured by TPO over the catalysts after 6 hours of reaction at 750°C and a CH_4/O_2 ratio of 2

Catalyst	Amount of carbon deposition (%)	CH_4 conversion at 6hrs
Ni/CZO	18.53	98.47
Ni-1%Mg/CZO	12.38	97.99
1%Mg-Ni/CZO	10.97	96.21
Ni-3%Mg/CZO	7.92	96.38
3%Mg-Ni/CZO	5.74	96.48

The amounts of carbon deposition on the catalysts after a reaction time of 6 hours at 750°C and a CH_4/O_2 ratio of 2 determined by TPO technique are shown in Table 4.3. The amount of carbon deposition on the Ni/CZO spent catalysts was 18.53 wt% whereas those of carbon deposition on the Ni-1%Mg/CZO , 1%Mg-Ni/CZO , Ni-3%Mg/CZO and 3%Mg-Ni/CZO spent catalysts were 12.38 , 10.97 , 7.92 and 5.74 wt%, respectively. The carbon deposition was found in the order Ni/CZO > Ni-Mg/CZO > Mg-Ni/CZO. These results indicate that the adding of Mg promoter into Ni/CZO catalysts could form NiO-MgO solid solution and/or increase the interaction between Ni and Mg. Consequently, the strong interactions between Ni and Mg and/or NiO-MgO solid solution could prevent the agglomeration of NiO particles at high temperatures resulting in suppressing the carbon deposition on the catalysts.

As suggesting of Milberg (2010), who studied the influence of Mg on the C adsorption on Ni, C atoms adsorbed preferentially on Ni surface. The partial replacement of Ni^{2+} with Mg^{2+} leads to the decrease of the number of the strong acid sites improved the basicity of Ni/CZO catalyst which benefited to disfavor the accumulation of cabon on the acid sites of support.

In addition, the carbon deposition is easy to deposit on a larger ensemble of active Ni sites (Trimm *et al.*, 1999). The addition of MgO can prevent the sintering of NiO particles at high temperature confirmed by SEM images (Figure 4.11). Thus, the coke formation occurs more difficultly because no Ni particles become nuclei for coke formation.

The amounts of carbon deposition gradually decrease with an increase of Mg content. This might be due to the catalyst with higher Mg promoter had the higher basicity, consequently benefited more efficiency to suppress carbon deposition (Yejun *et al.*, 2007).

Compared with coke formation over Ni-Mg/CZO and Mg-Ni/CZO, shorter filament and less amount of coke were found in Mg-Ni/CZO. This is in agreement with lower amount of weak or free NiO species measured by TPR technique (figure 4.4) because free NiO species, which has weak interaction with support, is responsible for coke formation (Roh *et al.*, 2007). One possible explanation of the effect of impregnation sequence is the more partially covering of NiO particles with MgO leading when the Ni^{2+} ion is deposited first.